58.0 Understanding Microstructure Evolution of High Temperature Ni Alloys Across Additive Manufacturing Processes

Juan Gonzalez (Mines)
Faculty: Jonah Klemm-Toole (Mines)
Collaborator: Andrew Wessman (University of Arizona)

This project initiated in Spring 2022. The research performed during this project will serve as the basis for a MS thesis program for Juan Gonzalez.

58.1 Project Overview and Industrial Relevance

Additive manufacturing (AM), a layer-by-layer deposition process, is a new manufacturing process that can revolutionize how we produce parts and products in many different industries. Among the different types of AM processes, Laser Powder Bed Fusion (LPBF) and Wire Arc Additive Manufacturing (WAAM) are some of the most commonly used techniques for the production of power industry components. Each AM process provides different benefits related with metal high deposition rates and geometric complexity opening a window to the fabrication of lower manufacturing cost of quality structural components compared to traditionally manufacturing manufactured counter parts (Subtracting Manufacturing), and also, allowing onsite fabrication of power plant replacement parts, preventing power plant outages that are expensive and deteriorate the robustness of the energy infrastructure [58.1].

We seek to explore and understand the annealing behavior of two Ni based alloys, Inconel 625 (solution strengthened alloy) and Haynes 282 (precipitation hardened), manufactured with WAAM and LPBF. Understanding the effect of AM process type on the microstructure of Ni based alloys is envisioned to open doors to improve the quality of manufactured components.

58.2 Previous Work

58.2.1 Literature Review and Background

Some investigations focused on the use of AM Nickel based alloys have evaluated different properties of manufactured components demonstrating that the properties of these alloys strongly depend on the final microstructure which can be controlled by the type of manufacturing technique and process [58.2]. The manufacture of power generation components using Nickel based alloys is always accompanied by heat treatments with the goal of dissolving or controlling precipitated undesirable embrittling phases such as borides, carbides and σ phases that form during solidification and subsequent thermal cycling. Previous work for this topic has suggested that it is necessary to reach the highest carbide solvus temperature to get recrystallization. However, the annealing response should be affected by the stored energy left in the material by the AM processes [58.3]. Therefore, an understanding of the effects of AM processes on the annealing behavior of Nickel based alloys either solid solution strengthened, or precipitation strengthened, is warranted.

58.2.2 Developing Experimental procedure.

To carry out this project, as-built and annealed samples were taken from IN625 and H282 metallic walls built with LPBF and WAAM for both nickel-based alloys using a collaborative robot (cobot) controlled Fronius CMT GMAW power source for WAAM. Two extra set of IN625 samples were made to study how the number of weld beads (one single dead = 1B, four weld beads = 4B) used on the manufacturing process would affect the annealing behavior of the alloy. Electron backscatter Diffraction (EBSD) was performed to compare the microstructural changes between as-built condition samples and the other specimens annealed during one hour at temperatures of 1000, 1100, and 1200ºC. Finally, microhardness testing was performed on the as-built condition and annealed specimens in order to evaluate how strength relates to the annealing response.

58.3 Recent Work

58.3.1 Microstructure Characterization

Inverse pole figure (IPF) maps taken on samples show columnar grain in the as-built condition for both alloys exhibiting notable differences on the amount, size, and grain distribution between the AM processes, as shown in **Figure 58.1**. As-built LPBF samples exhibit finer grains. Samples annealed at 1000 and 1100 ºC exhibited no recrystallization for both materials and AM processes. This is supported for the absence of annealing twins which are associated with recrystallization [58.4], **Figure 58.1(a)**. Although no recrystallization is observed after annealing at 1000 and 1100 °C, the gradual decrease in hardness after annealing, shown in **Figures 58.2** and **58.3**, indicate recovering is occurring. LPBF samples of both H282 and IN625 show complete recrystallization after annealing at 1200 °C, as shown in **Figures 58.1(a)** and **(b),** as well as exhibit a significant drop in hardness (**Figures 58.2** and **58.3).** It should be noted that although recrystallization occurs after annealing 1200 C, carbides are thermodynamically stable at this temperature for IN625 and H282, indicating that either these carbides are not effectives at preventing recrystallization, or they are not present in the microstructure.

None of the samples manufactured with WAAM recrystallized regardless of the annealing temperature, precipitates present, or the alloy tested. Additionally, all WAAM samples annealed at temperatures below 1200ºC exhibited similar hardness values from each other (and insignificantly different hardness values between multi pass and single pass welded samples), as shown in **Figure 58.2**. These results suggest that there is not enough stored energy in WAAM microstructures to induce recrystallization within the annealing temperatures investigated for IN625 and H282, promoting small microstructural changes after annealing. Though WAAM samples did not undergo recrystallization, they exhibited a hardness reduction proportional to the annealing temperature suggesting that the microstructure on these samples underwent recovery.

Despite large differences in hardness in the as-built condition, LPBF and WAAM samples show very similar hardness values, for a give alloy, after annealing at 1200 °C. It is interesting to note that although the recrystallized LPBF microstructures have quite difference grain sizes and morphologies to the non-recrystallized WAAM samples, the hardness values are comparable. This finding could indicate that WAAM microstructures are more suitable to long term high temperature applications compared to LPBF. For reference, **Figures 58.4(a)** and **(b)**, show main effect and interaction plots of the hardness data obtained thus far.

Unlike previous research works regarding the annealing behavior of Nickel-based alloys processed with AM, recrystallization in IN625 and H282 samples occurred below the highest carbide solvus temperature present in each alloy, indicating these phases do not control annealing behavior in additively manufactured samples, leading to conclude that differences in stored energy based on the additive manufacturing process has bigger effect on the annealing behavior than the equilibrium precipitates in the material.

58.4 Plans for Next Reporting Period

In the next reporting period, austenitic stainless steels including 316L, 316LSi, 316H, and 16-8-2 will be processed with WAAM to evaluate the influences of grain size and morphology on the kinetics of σ phase precipitation during extended exposures at 650 °C. Room temperature tensile testing will be used to assess the embrittling effects of σ phase precipitation.

8.5 References

[58.1] Wanwan Jin, Chaoqun Zhang, Shuoya Jin, Yingtao Tian, Daniel Wellmann and Wen Liu. Wire Arc Additive Manufacturing of Stainless Steels: A Review, in: Applied Sciences. MDPI, 2020, pp. 1–4.

[58.2] Apoorv Kulkarni. Additive Manufacturing of Nickel Based Superalloys, Houghton 49931USA

[58.3] Benjamin Graybill, Ming Li, David Malawey, Chao Ma, Juan-Manuel Alvarado-Orozco, Enrique Martinez-Franco. Additive manufacturing of nickel-based superalloys, MSEC2018-6666

[58.4] P. Poelt, C. Sommitsch, S. Mitsche, M. Walter. Dynamic recrystallization of Ni-base alloys-Experimental results and comparisons with simulations, Materials Science and Engineering A 420 (2006) 306–314

58.5 Figures

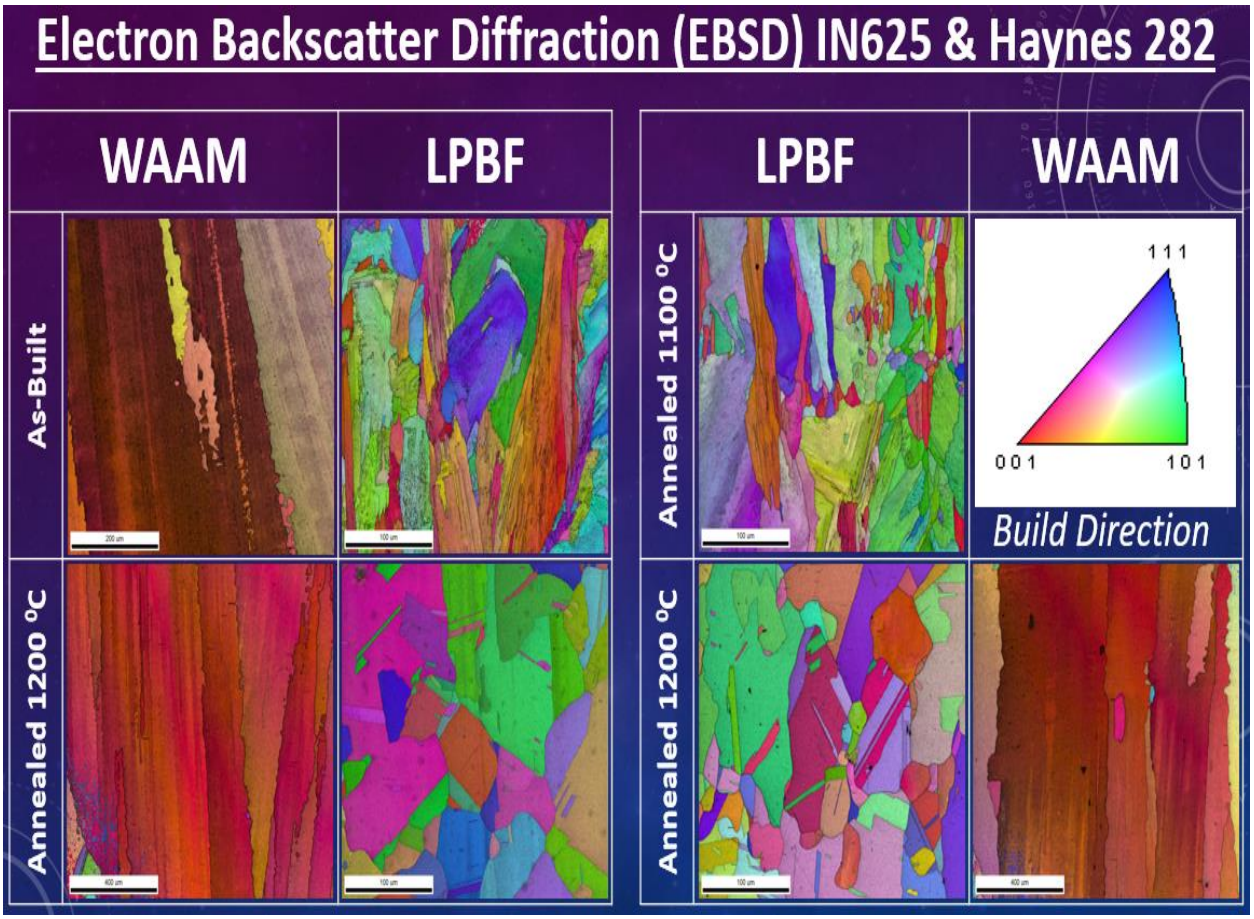

Figure 58.1. (a) Shows IN625 samples at different conditions, **(b)** Shows H282 samples at different conditions

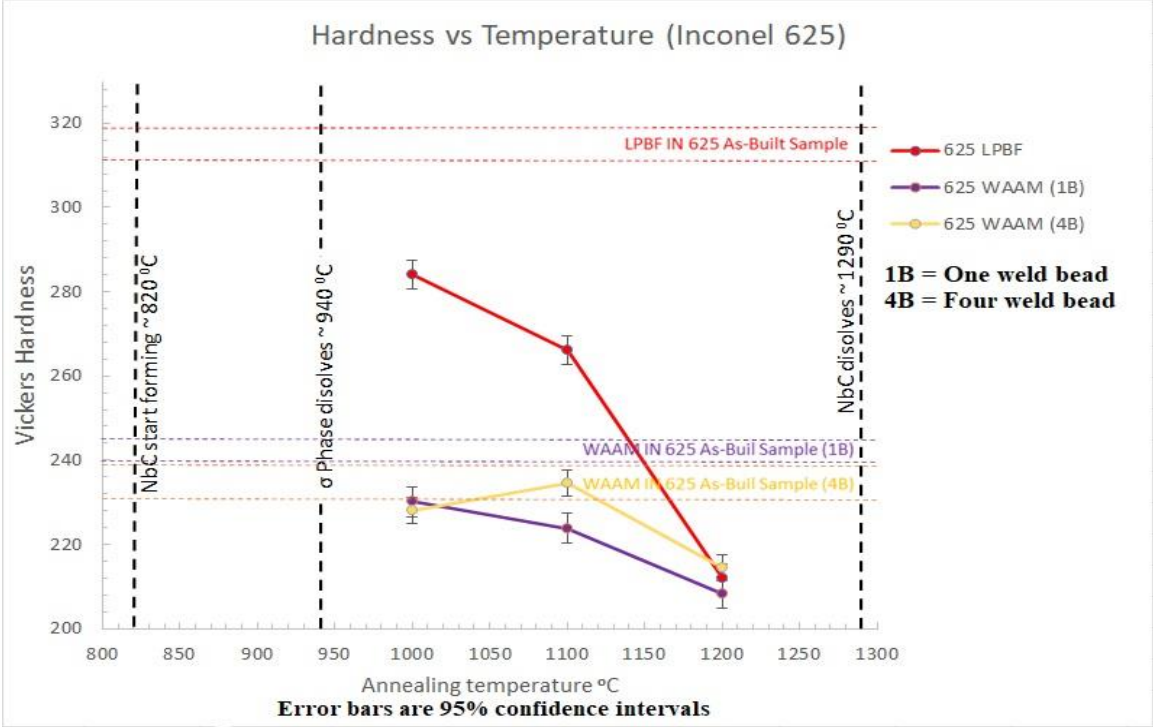

Figure 58.2. Vickers Hardness vs Annealing temperature plot of IN625 samples at different conditions, indicating the formation and dissolving temperatures of precipitates present in the alloy

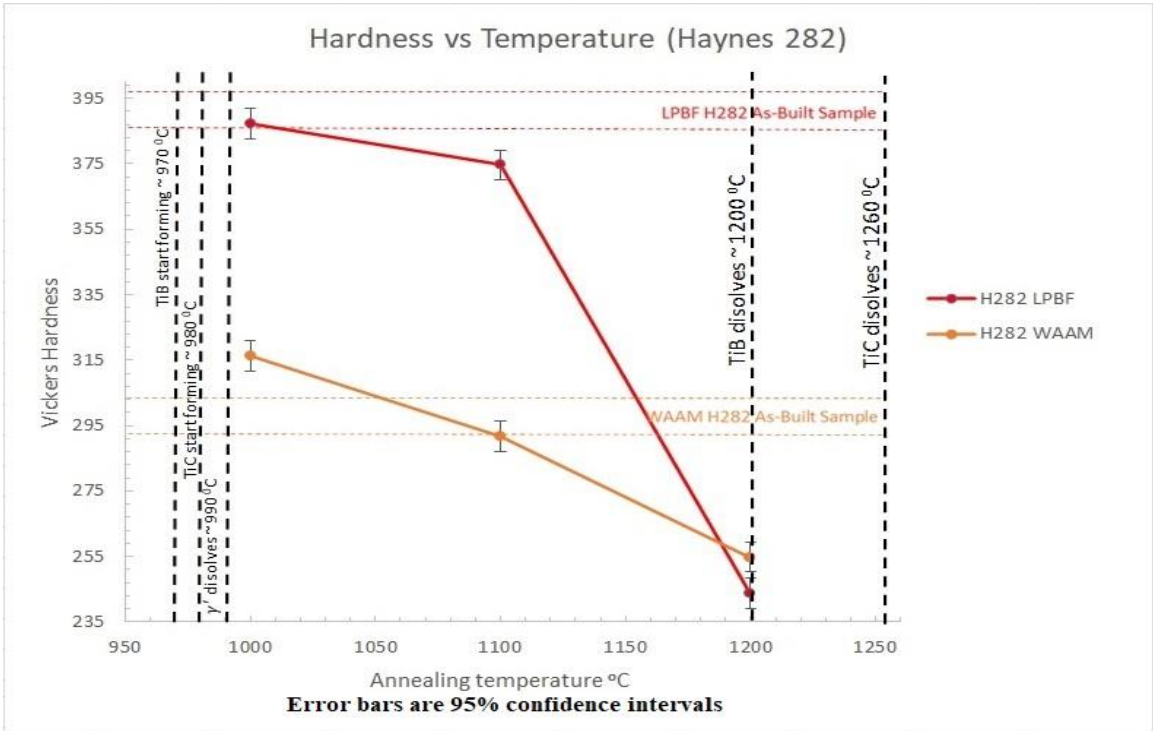

Figure 58.3. Vickers Hardness vs Annealing temperature plot of H282 samples at different conditions, indicating the formation and dissolving temperatures of precipitates present in the alloy

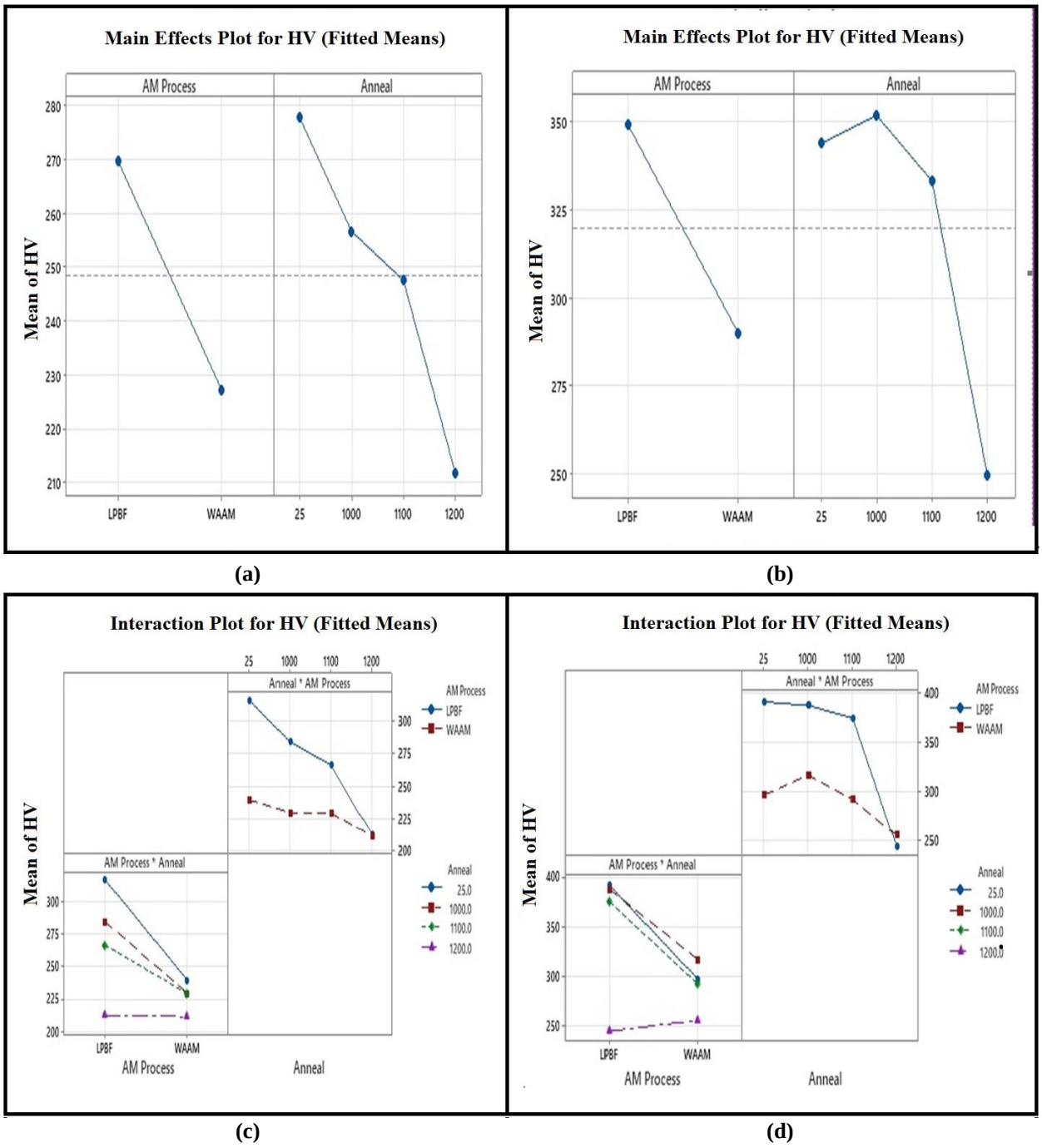

Figure 58.4. (a) IN625 Average hardness developed across AM processes (left) and annealing temperatures (right), **(b)** H282 Average hardness developed across AM processes (left) and annealing temperatures (right), **(c)** IN625 Interaction between AM processes and annealing temperatures, **(d)** H282 Interaction between AM processes and annealing temperatures